Available online at www.sciencedirect.com
ScienceDirect
European Journal of Medicinal Chemistry 43 (2008) 2238–2246
EUROPEAN JOURNAL OF MEDICINAL CHEMISTRY
http://www.elsevier.com/locate/ejmech

Original article

Studies of trypanocidal (inhibitory) power of naphthoquinones: Evaluation of quantum chemical molecular descriptors for structure–activity relationships

M. Paulino [a,*], E.M. Alvareda [a], P.A. Denis [a], E.J. Barreiro [b], G.M. Sperandio da Silva [b], M. Dubin [c], C. Gastellú [d], S. Aguilera [e], O. Tapia [f,**]

[a] *Department of Chemical Physics and Mathematics, Bioinformatics and Molecular Biomodelling Laboratory (DETEMA), Fac. Química. Gral. Flores 2124, 11600 Montevideo, Uruguay*
[b] *Laboratorio de Avaliaçao e Síntesis de Substancias Bioactivas (LASSBio), Faculdade de Farmácia, UFRJ, Rua Brigadeiro Trompowski-CCS-Bloco Bss Ilha do Fundão Ilha do Governador 21944190, CP 68024, Brazil*
[c] *Centro de Estudios Farmacológicos y Botánicos, CEFYBO-UBA-CONICET, Facultad de Medicina, 1121 Buenos Aires, Argentina*
[d] *Laboratorio Horus, Martin C. Martinez 2869, Montevideo, Uruguay*
[e] *Dept. Física, Lab. Crist. Mol., Fac. Ciencias, UCN, CC 1280, Antofagasta, Chile*
[f] *Department of Physical and Analytical Chemistry, Uppsala University, Box 579, S-751 23 Uppsala, Sweden*

Received 18 June 2007; received in revised form 12 December 2007; accepted 12 December 2007
Available online 6 January 2008

Abstract

Electronic, lipophilic and steric descriptors included in QSAR-2D and -3D are analyzed for a set of *ortho*- and *para*-naphthoquinones that have proved to be powerful oxidative agents with potent trypanocidal activities specially against *Leptomonas seymouri* and *Trypanosoma cruzi*. Electronic properties are calculated by means of semiempirical (PM3), ab initio (HF/3-21G) and density functional theory (B3LYP/6-31 + G*) methodologies. Three different electronic states, neutral quinones, hydroquinones and semiquinones, are studied to investigate if any one of them are statistically related with the biological activities. The best correlations were obtained at the B3LYP level of theory because it includes electronic correlation.

The QSAR-2D indicates that the best trypanocidal growth inhibitors are molecules in the semiquinone electronic state, with the following properties: (a) high negative value of E_{HOMO}, (b) high negative charge in the oxygen atoms of the carbonyl groups, (c) high positive charge in the carbon atom of one of carbonyl moieties and (d) high electronegativity (χ). In a complementary way, the QSAR-3D indicates that the electrostatic field correlates with trypanocidal activity and the presence of bulk moieties would increase activity.

The idea of comparing the three electronic states may prove to be of most importance in the general strategy to the design of new trypanocidal drugs. In fact, the experimental results showed that semiquinone is the one really statistically relevant indicating a clear connection between biochemical and theoretical aspects. Finally, we demonstrated that to be a good anti-trypanosomatid compound, the molecule must be a good electron acceptor to reach easily the essential semiquinone state. We expect that the present results motivate new experimental as well as theoretical investigations that confirm our findings.

Keywords: Quantum molecular descriptors; B3LYP; QSAR; Trypanosomatids; *o*-Naphthoquinones

Abbreviations: NADPH, reduced form of nicotinamide adenine dinucleotide phosphate; DTD, diaphorase; DTT, dithiotreitol; DHLA, dihydrolipoamide; LUMO, lowest unoccupied molecular orbital; HOMO, highest occupied molecular orbital; PCA, principal component analysis; PLS, principal least square; ROS, reactive oxygen species; QSAR-2D, two-dimensional quantitative structure–activity relationships; QSAR-3D, three-dimensional quantitative structure–activity relationships; CoMFA, comparative molecular field analysis; DFT, density functional theory; HF, Hartree–Fock; CGx, DRIMx, DHFNx, NTQx, quinone molecules which chemical formulae are described in text and in Figs. 1–3.

* Corresponding author. Tel.: +598 2 929 1558; fax: +598 2 924 7696.
** Corresponding author. Tel.: +46 184713659; fax: +46 184713654.
E-mail addresses: margot@fq.edu.uy (M. Paulino), orlando.tapia@fki.uu.se (O. Tapia).

0223-5234/$ - see front matter © 2007 Elsevier Masson SAS. All rights reserved.
doi:10.1016/j.ejmech.2007.12.023

1. Introduction

Quinones have been proposed as trypanocidal, cytostatic and antiviral agents [1–6]. The *o*-naphthoquinones, especially β-lapachone, α-lapachone, mansonones and analogues [7,8], are trypanosomatid growth inhibitors with high cytotoxic activity. By diverting reducing equivalents they inhibit microsomal lipid peroxidation [7,8]. Cytosolic and mitochondrial diaphorase (DTD), a quinone oxidoreductase, catalyzes quinones' reduction to hydroquinones via two mono-electronic steps. It has been demonstrated that, in a mixture of hepatic rat cytosol and β-lapachone (or the related *o*-naphthoquinones named in Fig. 1 as CGx (x = 10-248, 9-442, 8-935)), the *o*-naphthoquinones produced hydroquinones that in turn form the corresponding semiquinone and reactive oxygen species (ROS) [9,10] in a so-called oxidative comeback reaction. In another study, the quinones were reduced by ascorbate to semiquinones, followed by a mono-electronic transfer to dioxygen to yield superoxide anion radicals characterized as ROS.

However, in spite of the importance that quinones have in biological chemistry, only little is known about the characteristics of the mechanism that allows them to be good trypanocidal, cytostatic and antiviral agents. Since the mechanisms of reaction involving free radicals are grouped in three typical steps: initiation, propagation and termination (see Scheme 1), we investigated the three electronic states of the selected quinones to shed light into the mechanism of protection. For the later purpose we employed semiempirical, ab initio and DFT methodologies to determine the electronic and structural properties for the three states of the quinones. Then, a first quantitative structure–activity relationship (QSAR-2D) study with a first set of quinones (analogues of the β-lapachone) is performed to test if there is any particular electronic state (neutral quinone, hydroquinone or semiquinone) that would represent the active form of the population of *o*-naphthoquinones. Because quinones' molecular shape and local electronic properties are usually complementary to the active site of enzymes involved in the oxide-reduction metabolism, we add to our first *o*-naphthoquinone set, three more sets of *o*-naphthoquinones and *p*-naphthoquinones with variations in their shape as well as electronic properties. The structures of four sets are described in the following section and are used in a second QSAR (QSAR-3D (CoMFA)). We expect that the present results motivate new experimental as well as theoretical investigations that confirm our finding.

2. Methodology

2.1. Molecular systems, synthesis and bioassays

Many sets of *ortho*- and *para*-naphthoquinones have been reported [10–15]; the structures and biological data of that are used in this study.

A set of 11 *o*-naphthoquinones (Fig. 1) have been proved to be powerful oxidative agents with a well-known action mechanism, in which a semiquinone is an essential intermediate leading to superoxide anion in aerobic conditions (Scheme 1) [10]. All reported experimental biological data (DHLA, IC_{50} of *Leptomonas seymouri* and *Chritidia fasciculata*) are shown in Table 1.

The synthesis of another set of *p*-naphthoquinones (dihydronaphthofurandione and dihydrofuroquinolinedione derivatives) and the test for their trypanocidal activity in vitro against *Trypanosoma cruzi*, epimastigotes of Tulahuen strain, were reported [13–15]. Some of them have potent trypanocidal activities (Fig. 2).

Moreover, the synthesis and biological evaluation against *T. cruzi* Tulahuen strain of 10 new synthetic naphtho and anthraquinone sesquiterpene derivatives were described [14] and are shown in Fig. 2. Note that compounds DRIM1 and DRIM25 are more effective trypanocidal than nifurtimox.

Finally, the preparation of five naphtho[2,3-*b*]thiophen-4,9-quinone derivatives and the evaluation of their in vitro trypanocidal activities were reported [15]. NTQa and NTQd derivatives are most active against epimastigotes (Fig. 2).

2.2. Sampling for the quantitative structure–activity relationship studies

Five different kinds of samples were built:

SAMPLE I: the entire *o*-naphthoquinone samples in which each one of *o*-naphthoquinones are represented three times, each time in one of the three electronic states (semiquinone, neutral and hydroquinones). The size (*n*) of this sample is 33. Their chemical graphs and common names are shown in Fig. 1. The number of atomic positions is presented in Fig. 3.
SAMPLE IIH (n = 11): the 11 *o*-naphthoquinones of SAMPLE I (Fig. 1) in the hydroquinone electronic state.
SAMPLE IIS (n = 11): the 11 *o*-naphthoquinones of SAMPLE I (Fig. 1) in the semiquinone electronic state.
SAMPLE IIN (n = 11): the 11 *o*-naphthoquinones samples of SAMPLE I (Fig. 1) in the neutral electronic state.
SAMPLE III (n = 42): the 11 *o*-naphthoquinones of the SAMPLE IIN are put together with the 31 *p*-naphthoquinones presented in Fig. 2, conforming a sample of $n = 42$ molecules with which the QSAR-3D CoMFA analysis was performed.

2.3. Physicochemical properties

A procedure to model and geometry optimize the molecular structures was executed in three successive steps: (I) a computer assisted molecular model is obtained and its geometry refined using a molecular mechanics (MM+) [16] force field; (II) the geometry is improved to the extent that energy, as calculated by means of semiempirical (PM3) [17] and ab initio methods (HF/3-21G), comes to the corresponding stationary values when starting from a deformed geometry; (III) these geometries are re-optimized within density functional theory (DFT). In these last calculations, the B3LYP density function

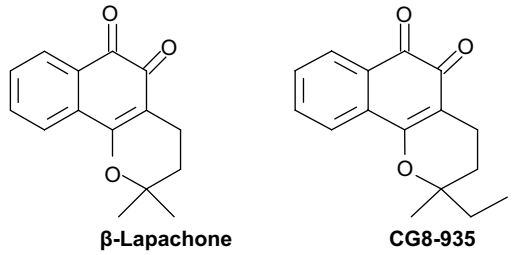

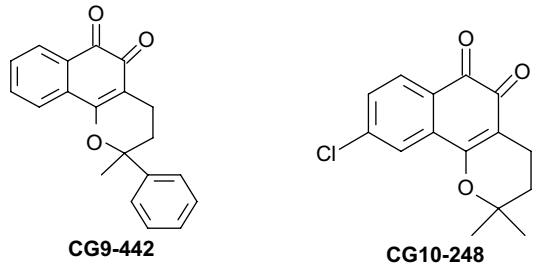

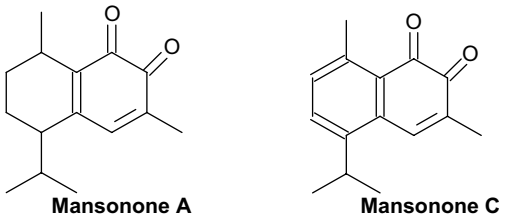

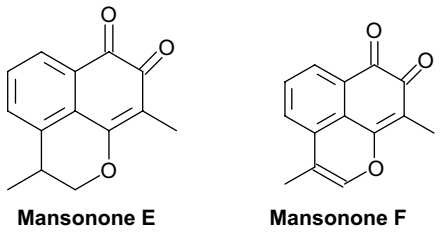

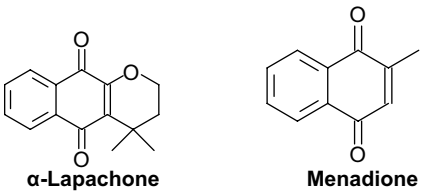

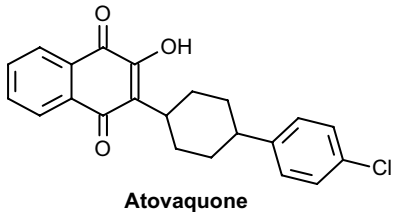

Total reaction:

$$DHLA + Q \rightarrow LA \text{ (disulfide lipoamide)} + QH_2$$

Initiation:

$$DHLA + Q \rightarrow DHLA\ (S\text{-}S^{\ominus\cdot}) \text{ (disulfide anion radical)} + Q^{\ominus\cdot} \text{ (semiquinone anion radical)}$$

Then the initiation continues until forming the disulfide LA and QH_2.

Propagation:

$$Q^{\ominus\cdot} + O_2^{\ominus\cdot} + 2H^+ \rightarrow QH_2 + O_2$$
$$2\,Q^{\ominus\cdot} + 2H^+ \rightarrow QH_2 + Q$$
$$Q^{\ominus\cdot} + H_2O_2 \rightarrow QH_2 + O_2^{\ominus\cdot}$$
$$Q + O_2^{\ominus\cdot} \rightarrow Q^{\ominus\cdot} + O_2$$

Termination:

$$Q^{\ominus\cdot} + Q^{\ominus\cdot} + 4H^+ \rightarrow 2QH_2$$
$$Q^{\ominus\cdot} + O2^{\ominus\cdot} + 2H^+ \rightarrow Q + H_2O_2$$
$$O_2^{\ominus\cdot} + O_2^{\ominus\cdot} + 2H^+ \rightarrow H_2O_2 + O_2$$

Scheme 1. Initiation, propagation and termination steps involved in the quinones reactivity.

employed includes the three parameter potential B3 developed by Becke [18] and the correlation potential LYP of Lee et al. [19]. Pople's 6-31 + G* basis set is used [20]. B3LYP optimizations were performed by means of Gaussian 98 program [21] using normal convergence criteria. Vibrational frequencies were determined analytically for all the molecules except atovaquone given that it is a too big-sized radical. In all cases, the structures were checked to correspond to potential energy minima, as indicated by positive force constants. Atomic charges (Q) were determined by fitting to the electrostatic potential according to Chrilian and Francl [22].

2.4. QSAR-2D

Quantitative structure–activity relationship (QSAR-2D) studies are based on an extra thermodynamic treatment which takes into account that each part of the molecule has influence on the equilibrium constant and the reaction rate of their chemical, biochemical and biological reactions, according to the variation in electronic, steric and lipophilic properties [23]. The QSAR study finishes once an equation is obtained where the activity of molecules is expressed as a combination (in our case, a linear combination) of the molecular descriptors for the electronic, steric and lipophilic properties of molecules. The QSAR-2D were made taking as the dependent variables the capacity to be reduced by dithiothreitol (DTT), the

Fig. 1. First set of studied quinone chemical structures. Abbreviations and chemical terms used are: β-lapachone, 3,4-dihydro-2,2-dimethyl-2*H*-naphtho[1,2-*b*]pyran-5,6-dione; α-lapachone, 3,4-dihydro-2,2-dimethyl-2*H*-naphtho[2,3-*b*]pyran-5,10-dione; CG8-935, 3,4-dihydro-2-methyl-2-ethylnaphtho[1,2-*b*]pyran-5,6-dione; CG9-442, 3,4-dihydro-2-phenyl-2-ethylnaphtho[1,2-*b*]pyran-5,6-dione; CG10-248, 3,4-dihydro-2-2-dimethyl-9-chloro-2*H*-naphtho[1,2-*b*]pyran-5,6-dione; mansonone A, 5,6,7,8-tetrahydro-3,8-dimethyl-5-isopropyl-1,2-naphthoquinone; mansonone C, 3,8-dimethyl-5-isopropyl-1,2-naphthoquinone; mansonone E, 2,3-dihydro-3,6,9-trimethyl-naphtho[1,8-*bc*]pyran-7,8-dione; mansonone F, 3,6,9-trimethyl-naphtho[1,8-*bc*]pyran-7,8-dione; menadione, 2-methyl-1,4-naphthoquinone; atovaquone, 2-[*trans*-4-(4′-chlorophenyl)cyclohexyl]-3-hydroxy-1,4-naphthoquinone.

Table 1
Effect of quinones on DHLA and DTT measured as oxygen consumption [9] and growth inhibition of *L. seymouri* and *C. fasciculata* [10]

Quinone (50 μM)	DTT (μM/min)	DHLA (μM/min)	IC_{50} (μM)	
			L. seymouri	*C. fasciculata*
α-Lapachone	1	7	4.1	27.0
β-Lapachone	238	808	0.4	–
CG10-248	470	879	0.4	0.8
CG9-442	315	990	0.7	0.7
CG8-935	208	733	0.3	0.8
Mansonone A	37	26	8.5	15.0
Mansonone C	–	434	4.0	6.0
Mansonone E	66	276	0.4	0.6
Mansonone F	14	58	0.1	0.3

capacity to be reduced by the dihydrolipoamide (DHLA), the growth inhibition of L. seymouri or the growth inhibition of C. *fasciculata* (Table 1) [24,25].

The frontier orbital energies, the lowest unoccupied molecular orbital (LUMO) and the highest occupied molecular orbital (HOMO) [26] and the partial net charges [27] for each atom were used as QSAR-2D electronic descriptors; of course, the final net charges were calculated using the lowest energy conformation obtained at the B3LYP/6-31 + G* level of calculation.

Additionally, polarizability [28], $\log P$ [29], and surface area were calculated using Hyperchem 6.0 [30]. The hardness (η) and the electronegativity (χ) were calculated in terms of the energies of the frontier orbitals HOMO and LUMO following Koopman's theorem Eqs. (1) and (2) [11–14].

$$\chi \cong -1/2(E_{\mathrm{HOMO}} + E_{\mathrm{LUMO}}) \quad (1)$$

$$\eta \cong -1/2(E_{\mathrm{HOMO}} - E_{\mathrm{LUMO}}) \quad (2)$$

The left-hand symbols are well-known chemical quantities; left-hand quantities depend upon the level of theory used. The hardness is a measure of the ionicity of an atom or molecule while its inverse, $1/\eta$ named chemical softness, measures the electronic polarizability of the system. These variables, in a multi-regression analysis, would take care of response properties involving the whole system to be docked [11–14]. For the present study, the more simple numeric approach has been selected due to the lack of definite structural knowledge on the receptor site.

Both dependent and independent variables were then included in a data set with which a QSAR-2D was made using a principal components analysis (PCA) procedure [31] in the Unscrambler 8.0 program [32].

An analysis of the correlation matrix was done by means of the regression model principal least square (PLS) version 2 [33]. The PLS method is used for relating the variations in one or several response variables (*Y*-variables) to the variations of several predictors (*X*-variables). To validate the models, the leverage correction is employed; this is a method to simulate model validation without performing any actual prediction. This model is based on the assumption that samples with a higher leverage (i.e. high influence on the model) will be predicted with less accuracy than samples with lower leverage. Thus a validation sample residual variance is computed from the calibration sample residuals, using a correction factor that increases with the sample leverage. All samples with low leverage (i.e. low influence on the model) will have estimated prediction residuals very close to their calibration residuals (the leverage being close to zero). From PLS2 model, a QSAR-2D equation is obtained; this is presented and discussed in Sections 3 and 4, respectively.

2.5. QSAR-3D

A second quantitative structure–activity relationship procedure (QSAR-3D/CoMFA) is performed by means of Sybyl 6.8 software [34]. This methodology represents the molecules by steric (Lennard–Jones) [35] and electrostatic (Coulomb) fields, calculated with a probe charge over the 3D molecular surface.

In the first step of the CoMFA procedure, a common substructure, the naphthalene ring, was selected as pharmacophore and used as template to do an alignment of all sample molecules.

The resulting CoMFA data are analyzed with a PLS method and the resulting model is validated by means of both internal and external cross-validation procedures. The internal validation can be determined through the value of the cross-validated q^2 (cross-validation correlation coefficient) reported by PLS, using the 70% of data. In this method some samples are kept out of the calibration and are used for prediction. This is repeated until all samples have been kept out once. The external validation, calculated as in Ref. [36], uses a predictive r^2 value, retaining the 30% of data:

$$r^2_{\mathrm{pred}} = (1 - \mathrm{SSD})/\mathrm{PRESS} \quad (3)$$

where SSD is the sum of squared deviation from the mean and PRESS is the sum of squared differences between the actual and the predicted values.

3. Results

3.1. QSAR-2D of the o-naphthoquinone set

A statistical study comparing significance of the semiempirical, HF/3-21G and B3LYP/6-31 + G* methodologies was performed by means of PCA and regression analysis of SAMPLE I (Table 2). For the regression analysis presented, seven PCs were taken into account together with a PLS2 method using as dependent variables those previously described (DTT, DHLA, IC_{50} of *L. seymouri*).

Once all regression analyses are done, the best model is that in which the *L. seymouri* activity correlates with the electronic variables calculated with B3YLP/6-31 + G* method. It is noticeable that when *C. fasciculata* is used as dependent variable, it was not possible to obtain models of good statistical quality. However, the semiempirical methods did not give good correlations. The model shows a big difference between the calibration and the validation

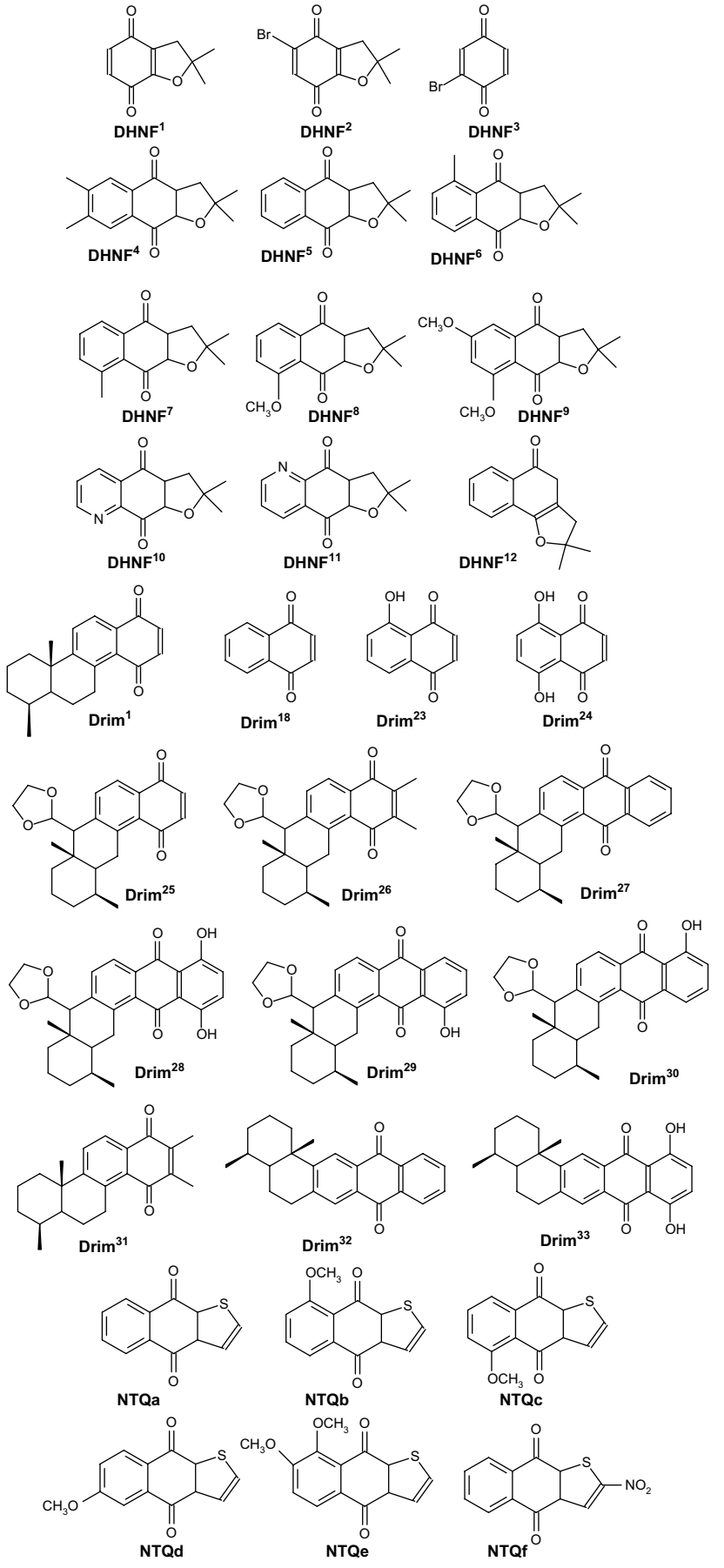
DHNF1
DHNF2
DHNF3
DHNF4
DHNF5
DHNF6
DHNF7
DHNF8
DHNF9
DHNF10
DHNF11
DHNF12
Drim1
Drim18
Drim23
Drim24
Drim25
Drim26
Drim27
Drim28
Drim29
Drim30
Drim31
Drim32
Drim33
NTQa
NTQb
NTQc
NTQd
NTQe
NTQf

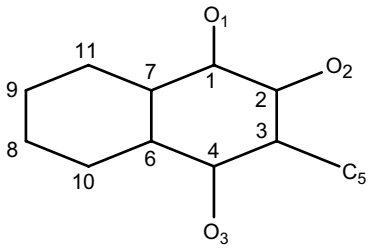

Fig. 3. Molecular model used in electronic calculations. The atoms of the quinones are numbered.

r^2 correlation coefficients. Nine variables in the PCA plot are placed in the outer ellipsoid (explaining the 100% of the model variance) and the other variables are inside the inner ellipsoid explaining the 50% of the variability. Employing the HF/3-21G* methodology did not improve the results. Therefore, the best fitting observed is with the DFT model ($r^2_{\text{calibration}} = 0.97$; $r^2_{\text{validation}} = 0.95$) because it includes correlation energy and the HF methodology does not.

In the following step of the statistical analysis, the three electronic quinone configurations (SAMPLE IIH, SAMPLE IIS and SAMPLE III) were studied separately. The best correlation was that found between IC_{50} of *L. seymouri* taken as dependent variable and the semiquinone population (Fig. 4 and Table 3). The statistical values obtained were $r^2_{\text{correlation}} = 1$; $r^2_{\text{prediction}} = 0.99$ and the resulting QSAR-2D equation is:

$$\begin{aligned} IC_{50}\,L.seymouri = {} & 76.274940 + 3.816 \log P - 0.504\text{Pola} \\ & + 21.373\, E_{\text{HOMO}} - 37.304\,\text{QC1} \\ & + 3.340\,\text{QC3} + 76.298\,\text{QO1} + 24.914\,\text{QO2} \\ & - 93.999\chi \end{aligned} \tag{4}$$

3.2. QSAR-3D of the o- and p-naphthoquinone sets

The SAMPLE III, integrating *ortho*- and *para*-naphthoquinones, is used to perform the comparative molecular field analysis (CoMFA).

Table 2
Regression results obtained for all quinones populations, using DITHIO, DHLA and IC_{50} of *L. seymouri* as the dependent variable vs the methods employed in this study

Methods	Regression coefficient for calibration model	Regression coefficient for validation model
Semiempirical	0.99	0.66
Ab initio	0.84	0.74
DFT	0.97	0.95

4. Discussion

4.1. QSAR-2D of the o-naphthoquinone set

As expressed above, the comparison of three statistical models (neutral, hydroquinone and semiquinone electronic states) using the B3LYP/6-31 + G* results have shown the best fitting for the semiquinone electronic state (SAMPLE IIS), taking IC_{50} of *L. seymouri* as dependent variable and E_{HOMO}, QC1, QC3, QO1, QO2, polarizability (Pola), log *P* and χ as independent variables (Fig. 4, Table 3 and Eq. (3))

For the molecule set assayed, E_{HOMO}, QO1 and QO2 have negative values; QC1 has positive values while QC3 may have either negative or positive values in the sample.

As validation test for Eq. (3), the IC_{50} of *L. seymouri* was calculated and compared with experimental values (Table 4). Using the same equation, the predicted values for the radicals of menadione and atovaquone are 11.4 μM and 2.8 μM, respectively, predicting that atovaquone could result in a better anti-*L. seymouri* agent than menadione because it has more acceptable hydrophobicity, polarizability, frontier orbital and charge descriptors (cf. Eq. (3)).

4.2. QSAR-3D of the o- and p-naphthoquinones, SAMPLE III

The data from the CoMFA model are analyzed with the above-mentioned PLS method; the resulting model is validated by means of both internal and external cross-validation procedures. The results are graphically represented as a 3D

Fig. 2. Set of dihydronaphthofurandiones and dihydrofuroquinolinediones (DHNFx), drimane quinones (Drimx) and naphtho[2,3-*b*] thiophen-4,9-quinones (NTQx) used in the CoMFA analysis. Abbreviations and chemical terms used are: DHFN1, 2,3-dihydrobenzo[*b*]furan-4,7-dione; DHFN2, 5-bromobenzofurandione; DHFN3, 6-bromobenzofurandione; DHFN4, 2,3-dihydro-2,2,6,7-tetramethylnaphtho[2,3-*b*]furan-4,9-dione; DHFN5, 2,3-dihydro-2,2,-dimethylnaphtho[2,3-*b*] furan-4,9-dione; DHFN6, 2,3-dihydro-2,2,5-trimethylnaphtho[2,3-*b*]furan-4,9-dione; DHFN7, 2,3-dihydro-2,2,8-trimethylnaphtho[2,3-*b*]furan-4,9-dione; DHFN8, 2,3-dihydro-8-methoxy-2,2-dimethylnaphtho[2,3-*b*]furan-4,9-dione; DHFN9, 2,3-dihydro-6,8-dimethoxy-2,2-dimethylnaphtho[2,3-*b*]furan-4,9-dione; DHFN10, 2,3-dihydro-2,2-dimethylfuro[3,2-*g*]quinoline-4,9-dione; DHFN11, 2,3-dihydro-2,2-dimethylfuro[2,3-*g*]quinoline-4,9-dione; DHFN12, 2,3-dihydro-2,2-dimethylnaphtho[1,2-*b*]furan-4,5-dione; DRIM1, (+)-(4a*S*,12b*S*)-4,4,12b-trimethyl-1,2,3,4,4a,5,6,12b-octahydrobenzo[*a*]anthracene-8,11-dione; DRIM18, 1,4-naphthoquinone; DRIM23, 5-hydroxy-1,4-naphthoquinone (Juglone); DRIM24, naphthazarin, 5,8-dihydroxy-1,4-naphthoquinone; DRIM25, (−)-(7*R*, 7a*S*,11a*S*)-7-[1,3]dioxolan-2-yl-7a,11,11-trimethyl-7,7a,8,9,10,11,11a,12-octahydrobenzo[*a*]anthracene-1,4-dione; DRIM26, (−)-(7*R*,7a*S*,11a*S*)-7-[1,3]dioxolan-2-yl-2,3,7a,11,11-pentamethyl-7,7a,8,9,10,11,11a,12-octahydrobenzo[*a*]-anthracene-1,4-dione; DRIM27, (−)-(8*R*,8a*S*,12a*S*)-8-[1,3]dioxolan-2-yl-8a,12,12-trimethyl-8,8a,9,10,11,12,12a,13-octahydro-pentaphene-5,14-dione; DRIM28, (−)-(8*R*,8a*S*,12a*S*)-8-[1,3]dioxolan-2-yl-1,4-dihydroxy-8a,12,12-trimethyl-8,8a,9,10,11,12,12a,13-octahydro-pentaphene-5,14-dione; DRIM29, (−)-(8*R*,8a*S*,12a*S*)-8-[1,3]dioxolan-2-yl-1-hydroxy-8a,12,12-trimethyl-8,8a,9,10,11,12,12a,13-octahydro-pentaphene-5,14-dione; DRIM30, (−)-(8*R*,8a*S*,12a*S*)-8-[1,3]dioxolan-2-yl-4-hydroxy-8a,12,12-trimethyl-8,8a,9,10,11,12,12a,13-octahydro-pentaphene-5,14-dione; DRIM31, (+)-(4a*S*,12b*S*)-4,4,9,10,12b-pentamethyl-1,2,3,4,4a,5,-6,12b-octahydrobenzo[*a*]anthracene-8,11-dione; DRIM32, (+)-(4a*S*,14b*S*)-4,4,14b-trimethyl-1,2,3,4,4a,5,6,14b-octahydrobenzo[*a*]naphthacene-8,13-dione; DRIM33, (+)-(4a*S*,14b*S*)-9,12-dihydroxy-4,4,14b-trimethyl-1,2,3,4,4a,5,6,14b-octahydrobenzo[*a*]naphthacene-8,13-dione; NTQa, naphtho[2,3-*b*]thiophen-4,9-quinone; NTQb, 8-methoxy-naphtho[2,3-*b*]thiophen-4,9-quinone; NTQc, 5-methoxy-naphtho[2,3-*b*]thiophen-4,9-quinone; NTQd, 6-methoxy-naphtho[2,3-*b*]thiophen-4,9-quinone; NTQe, 7,8-dimethoxy-naphtho[2,3-*b*]thiophen-4,9-quinone; NTQf, nitro-naphtho[2,3-*b*]thiophen-4,9-quinone [11–13].

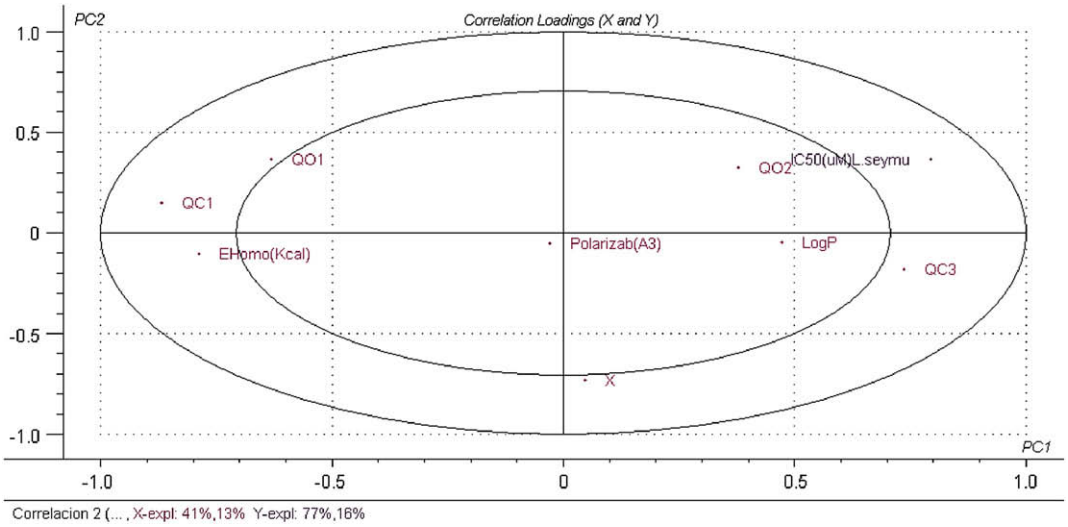

Fig. 4. PCA of semiquinones with DFT calculation. The significant variables appear between 50% and 100% of variability, represented by the two ellipsoids. The small ellipsoid explains the 50% of variability and the bigger one explains the 100% of the variability of the data.

plot in Figs. 5 and 6. The electrostatic field correlates with activity increase when positive ($\delta+$) on C1 and C2 and the negative ($\delta-$) on O1 and O2 charges augment while decreasing the $\%IC_{50}$ in epimastigotes. The so-called steric field shows that a substitution with bulk moieties might increase the activity. Both results, in accordance with those of QSAR-2D, reinforce the hypothesis of electronic influence of the carbonyl moieties in the proposed mechanism.

Statistical parameters of the best CoMFA were $r^2 = 0.968$, $F = 72.991$ and the estimated standard error was 0.245 indicating that the model has a good predictive ability.

For the dihydronaphthofurandione and dihydrofuroquinolinedione derivatives [11–14], the presence of a pyridine enhanced the trypanocidal activity when this one was correlated to electroaffinity and the electronegativity of the molecules. Also for the DRIMx [15], it is noted that the most important region responsible for the tripanocidal activity is the presence of an unsubstituted region 2–3 near one of the carbonyl groups.

5. Conclusions

In the PCA study of the entire *o*-naphthoquinones, SAMPLE I (Fig. 1), the best regression parameters were obtained when the IC_{50} of *L. seymouri* activity was used as dependent variable and the DFT descriptors as independent variables. The correlation for the calibration was 0.97 and for the validation was 0.95 (Table 2).

When the quinones were grouped into three different samples (neutral, semiquinones and hydroquinones; SAMPLE IIN, SAMPLE IIS and SAMPLE IIH) the same procedure is applied and new regression analysis performed. The values obtained for the radicals showed the best correlation with respect to the dependent variable. When the electronic properties were evaluated by means of the DFT methodology and IC_{50} of *L. seymouri* as dependent variable (Table 3), the statistic model evaluation indicated that the *semiquinones* (SAMPLE IIS) generated the best model. Indeed, the best correlation obtained was 1.00 for the calibration and 0.99 for the validation. With these results, we propose an action mechanism in which the active form of *o*-naphthoquinones' population (Scheme 2) responsible for the redox mechanism and correspondingly for the capacity of growth inhibition should be the semiquinone. Further experimental as well as experimental investigations are required to confirm our idea.

In addition to this, the obtained QSAR-2D Eq. (3) predicts that the *L. seymouri* inhibitory growth activity of the SAMPLE IIS of semiquinones will be increased (and the IC_{50} value will decrease correspondingly) tuning the following factors:

(a) a more negative value of E_{HOMO},
(b) negative charge of atoms O1 and O2 increased,
(c) the increase of the positive charge QC1 and the increase of electronegativity (χ).

Table 3
Regression analysis for the different states of the quinones expressed with IC_{50} of *L. seymouri* as dependent variable

Method	Neutral quinones		Hydroquinones		Semiquinones	
	Correlation coefficient of calibration	Correlation coefficient of validation	Correlation coefficient of calibration	Correlation coefficient of validation	Correlation coefficient of calibration	Correlation coefficient of validation
Semiempirical	0.97	0.90	0.97	0.94	0.95	0.84
Ab initio	0.92	0.85	0.74	0.24	0.99	0.96
DFT	0.92	0.76	0.98	0.93	1.00	0.99

Table 4
Validation and predicted values for the first set of *o*-naphthoquinones

Quinone (50 μM)	IC_{50} (μM)	
	L. seymouri	*L. seymouri*, predicted
α-Lapachone	4.1	4.1
β-Lapachone	0.4	0.4
CG10-248	0.4	0.4
CG9-442	0.7	0.7
CG8-935	0.3	0.3
Mansonone A	8.5	8.5
Mansonone C	4.0	4.0
Mansonone E	0.4	0.4
Mansonone F	0.1	0.1
Menadione	–	11.4
Atovaquone	–	2.8

Thus, the present results can be also confirmed if the inhibitory growth activity is determined for quinones that have the properties above-mentioned.

The model predicts with 100% of agreement the experimental values for *o*-naphthoquinones. In consequence, it could be used to predict the anti-*L. seymouri* activity for menadione and atovaquone. In view of these results, it seems to be unnecessary to evaluate the experimental IC_{50} for atovaquone and menadione against *L. seymouri*: the model could be used to predict that value.

In agreement with the QSAR-2D best model, the QSAR-3D (CoMFA) models show that a substitution for negative moieties in the carbonyls region (C1, O1 and C2, O2) of the quinones will enhance the biological activity (*T. cruzi* growth inhibition %). However, a substitution for positive moieties will decrease the activity (blue field in Fig. 6). In the steric plot, the yellow colored field shows that bulk substituents at C3 and C5 would decrease activity; again according to the QSAR-2D model Eq. (4). A green field shows that in the positions of C9 and C11 bulk moieties would enhance the activity.

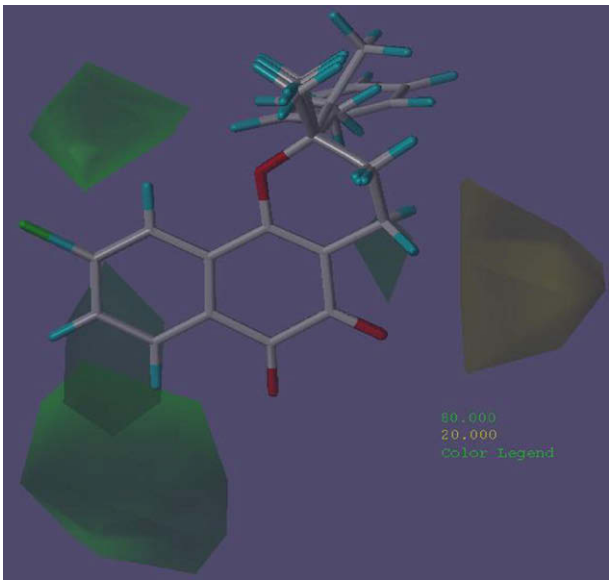

Fig. 6. CoMFA plot showing steric fields for the quinones used. The quinones are represented as sticks and steric field contours are represented in yellow and green colors. Green field is favorable to bulk substituents and yellow field is unfavorable to bulk substituents. (For interpretation of the references to color in this figure legend, the reader is referred to the web version of this article.)

All our results suggest that a charge transfer complex between a π-donor agent and the acceptor (the neutral quinone) could be formed through an electronic transfer to the frontier orbital HOMO of atoms O1 or O2 by the interaction of the carbonyl (C1═O1 or C2═O2); additionally this is to be favored by an interaction between both C1═O1 and C2═O2. This conclusion opens a possibility to develop further and specialized studies of a possible charge transfer role. Indeed, Molfetta et al. [37] found that ‘‘some active anti-trypanocidal compounds are not good electron-donor molecules when compared with the inactive ones’’. This observation is in absolute coincidence with ours. This statement is to be taken in the

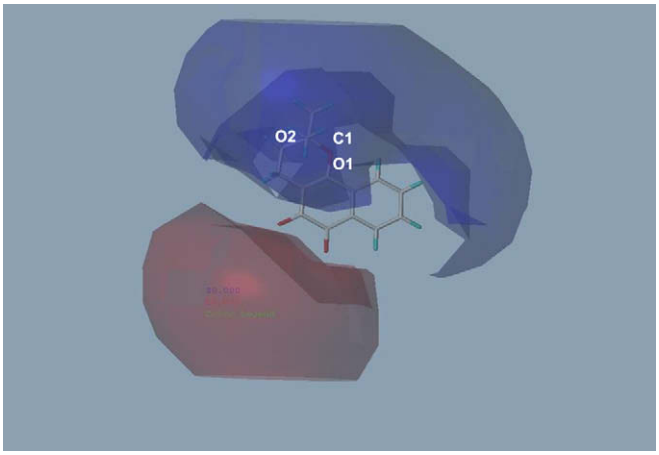

Fig. 5. CoMFA plot showing electrostatic fields for the quinones used. The quinone molecule is represented as sticks and the electronic field contours are represented in blue and red colors. Red field is favorable to negative substituents and blue field is favorable to positive substituents. (For interpretation of the references to color in this figure legend, the reader is referred to the web version of this article.)

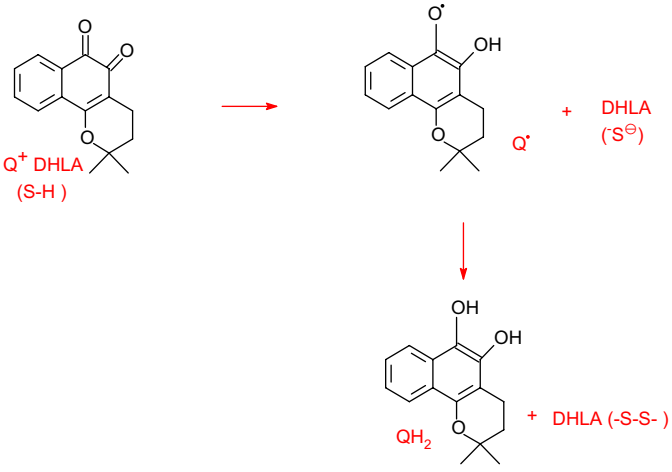

Scheme 2. Quinones action mechanism [3]. Q = quinones; DHLA = dihydrolipoamide; QH2 = hydroxy quinone; LA = lipoamidedisulfide; Q• = semiquinone free radical. DHLA (S–H) reduces the quinone into hydroxy quinone and at the same time the disulfide lipoamide DHLA (S–S) is formed. In an intermediate step the semiquinone and the radical disulfide anion DHLA (–S) is formed [19].

sense that we demonstrate that, to be a good anti-trypanosomatid compound, the molecule must be a good electron acceptor to reach easily the essential semiquinone state.

With the natural limitations that this work may have, the idea of comparing the three electronic states and the experimental results showing that it is the semiquinone the one really statistically relevant seems to be a valuable approach. The choice of theoretical method plays also a key role. The results indicate a clear connection between biochemical and theoretical aspects by pinpointing which electronic state might be the crucial one. The observation that the experimental data with the semiquinones gives the best fit strongly suggests that they might be the key form of the quinones for the bioactivity and could be a probe for the mechanism of action.

The obtained QSAR-2D equation gives a tool to predict activities and could stimulate experimentalist to synthesize new compounds with the aim to integrate this information in a general strategy to the discovery of new and less toxic anti-trypanosomatid drugs.

Acknowledgements

This work was supported by the ChagaSpace project, LFMMB, Fac. Química. Gral. Flores 2124, 11600 Montevideo, Uruguay. MP and MD thanks AUGM (Asociación de Universidades Grupo Montevideo).

References

[1] A. Pinto, V. Ferreira, R. Capella, B. Gilbert, M. Pinto, Trans. R. Soc. Trop. Med. Hyg. 81 (1987) 609–610.
[2] S.M. Planchon, J.J. Pink, K.A. Robertson, W.G. Bornmann, Oncol. Rep. 6 (1999) 485–492.
[3] B. Frydman, L.J. Marton, J.S. Sun, K. Neder, D.T. Witiak, A.A. Liu, H.-M. Wang, Y. Mao, H.-Y. Wu, M.M. Sanders, L.F. Liu, Cancer Res. 57 (1997) 620–627.
[4] M.E. Dolan, B. Fridman, C.B. Thompson, A.M. Diamond, B.J. Garbiras, A.R. Safa, W.T. Beck, L.J. Barton, Anticancer Drugs 9 (1998) 437–448.
[5] A. Vanni, M. Fiore, A. De Salvia, E. Cundari, R. Ricordy, R. Ceccarelli, F. De Grassi, Mutat. Res. 401 (1998) 55–61.
[6] S.M. Wuerzberger, S.M. Planchon, K.L. Byers, W.G. Bornmann, D.A. Bothman, Cancer Res. 58 (1998) 1876–1885.
[7] M. Dubin, S. Fernández Villamil, A.O.M. Stoppani, Biochem. Pharmacol. 39 (1990) 1151–1160.
[8] S. Fernandez Villamil, M. Dubin, C. Galeffi, A.O.M. Stoppani, Biochem. Pharmacol. 40 (1990) 2343–2351.
[9] S. Fernandez Villamil, Andres O.M. Stoppani, M. Dubin, Redox cycling of β-lapachone and structural analogues in microsomal and cytosol preparations, Quinones and Quinone Enzymes, In: Methods in Enzymology, vol. 37 (2004) 67–87.
[10] M. Paulino, M. Hansz, N. Hikichi, G. Tabares, M.P. Molina Portela, S.H. Fernandez Villamil, C.M. Sreider, A.O.M. Stoppani, An. Asoc. Quim. Argent. 82 (1994) 371–389.
[11] P. Perez, R. Contreras, A. Vela, O. Tapia, Chem. Phys. Lett. 269 (1997) 419–427.
[12] P. Geerlings, F. De Proft, W. Langenaeker, Chem. Rev. 103 (2003) 1793–1873.
[13] R.A. Tapia, C. Salas, A. Morello, J.D. Mayab, A. Toro-Labbé, Bioorg. Med. Chem. 12 (2004) 2451–2458.
[14] M.A. Cuellar, C. Salas, M.J. Cortes, A. Morillo, J.D. Maya, M.D. Preite, Bioorg. Med. Chem. 11 (2003) 2489–2497.
[15] C.L. Zani, E. Chiari, A.U. Krettli, S.M.F. Murta, M.L. Cunningham, A.H. Fairlamb, A.J. Romanha, Bioorg. Med. Chem. 5 (1997) 2185–2192.
[16] N.L. Allinger, J. Am. Chem. Soc. 99 (1977) 8127.
[17] J.P. Stewart, J. Comput. Chem. 10 (1989) 209–220.
[18] A.D. Becke, J. Chem. Phys. 98 (1993) 5648.
[19] C. Lee, W. Yang, R.G. Parr, Phys. Rev. B 37 (1988) 785.
[20] W.J. Hehre, L. Radom, P.v.R. Schleyer, J.A. Pople, Ab initio Molecular Orbital Theory, Wiley, New York, 1986.
[21] M.J. Frisch, G.W. Trucks, H.B. Schlegel, G.E. Scuseria, M.A. Robb, J.R. Cheeseman, V.G. Zakrzewski, J.A. Montgomery Jr., R.E. Stratmann, J.C. Burant, S. Dapprich, J.M. Millam, D. Daniels, K.N. Kudin, M.C. Strain, O. Farkas, J. Tomasi, V. Barone, M. Cossi, R. Cammi, B. Mennucci, C. Pomelli, C. Adamo, S. Clifford, J. Ochterski, G.A. Petersson, P.Y. Ayala, Q. Cui, K. Morokuma, D.K. Malick, A.D. Rabuck, K. Raghavachari, J.B. Foresman, J. Cioslowski, J.V. Ortiz, A.G. Baboul, B.B. Stefanov, G. Liu, A. Liashenko, P. Piskorz, I. Komaromi, R. Gomperts, R.L. Martin, D.J. Fox, T. Keith, M.A. Al-Laham, C.Y. Peng, A. Nanayakkara, C. Gonzalez, M. Challacombe, P.M.W. Gill, B. Johnson, W. Chen, M.W. Wong, J.L. Andres, C. Gonzalez, M. Head-Gordon, E.S. Replogle, J.A. Pople, Gaussian 98, Gaussian, Inc., Pittsburgh, PA, 1998.
[22] L.E. Chrilian, M.M. Francl, J. Comput. Chem. 8 (1987) 894.
[23] C.F.T. Hansch, J. Am. Chem. Soc. 86 (1963) 1616–1625.
[24] M.P. Molina Portela, A.O.M. Stoppani, Biochem. Pharmacol. 51 (1996) 275–283.
[25] M. Molina Portela, S. Fernandez Villamil, L.J. Perissinotti, A.O.M. Stoppani, Biochem. Pharmacol. 52 (1996) 1875–1882.
[26] K. Fukui, Nobel Lecture: The Role of Frontier Orbitals In Chemical Reactivities, vol. 2, The Nobel Foundation, 1981, Nobel Lectures in Chemistry 1981–1990. Bo.G. Malmström (Ed.) (Chalmers University Of Technology and Göteborg University, Sweden)147.
[27] R.S. Mulliken, J. Am. Chem. Soc. 74 (1952) 811.
[28] K.J. Miller, J. Am. Chem. Soc. 112 (1990) 8533.
[29] A.K. Ghose, A. Pritchett, G.M. Crippen, J. Comput. Chem. 9 (1988) 80–90.
[30] Hyperchem 6.0 to Windows, Hypercube, Inc., 2000.
[31] K. Esbensen, P. Geladi, Chemometrics and intelligent laboratory systems (1987) pp. 37–52.
[32] CAMO, S.I.P.L. In Copyright © CAMO PROCESS AS: Nedre Vollgate 8, N-0158, Oslo, Norway. #1056, 7th Main, HAL 2nd Stage, Indiranagar, Bangalore 560 038, India, 2003.
[33] H. Martens, M.M, Proceedings of International Symposium on PLS Methods, Paris, 5–6 October 1999.
[34] Tripos, Tripos Associates, St. Louis (MO), 2003.
[35] D. Richard, I. Cramer, D.E. Patterson, J.D. Bunce, J. Am. Chem. Soc. 110 (1988) 5959–5967.
[36] G.M.S. Silva, C.M.R. Sant'Annaa, E.J. Barreiro, Bioorg. Med. Chem. 12 (2004) 3159–3166.
[37] F.A. Molfetta, A.T. Bruni, K.M. Honorio, A.B.F. da Silva, Eur. J. Med. Chem. 40 (2005) 329–338.